Astrodynamic Calculations and 3-Dimensional Model of a Vasimr Engine Powered Spacecraft for the Accelerated Transportation of Small Spacecraft to Mars

A project present to
The Faculty of the Department of Aerospace Engineering
San Jose State University

in partial fulfillment of the requirements for the degree
Master of Science in Aerospace Engineering

By

Gustavo Moreno

May, 2017

approved by

Dr. Kamran Turkoglu
Faculty Advisor

The Designated Project Advisor/Committee Approves the Project Titled

ASTRODYNAMIC CALCULATIONS AND 3-DIMENSIONAL MODEL
OF A VASIMR ENGINE POWERED SPACECRAFT
FOR THE ACCELERATED TRANSPORTATION
OF SMALL SPACECRAFT TO MARS

by

Gustavo Moreno

APPROVED FOR THE DEPARMENT OF AEROSPACE ENGINEERING

SAN JOSE STATE UNIVERSITY

MAY 2017

Dr. Kamran Turkoglu Department of Aerospace Engineering

ABSTRACT

ASTRODYNAMIC CALCULATIONS OF A VASIMR ENGINE POWERED SPACECRAFT FOR THE ACCELERATED TRANSPORTATION OF SMALL SPACECRAFT TO MARS

by Gustavo Moreno

This paper explores and analyzes how various VASIMR engine configurations can affect the required travel time for a hypothetical spacecraft's mission to Mars. The efficiency of the engine will be demonstrated by comparing various computer generated simulations with the common Hohmann transfer approach. Various computer programs and 3-dimensional simulations will be designed and implemented through Matlab and Simulink software programs. Calculations will be performed with few assumptions in order to ensure some theoretical validity to the application of VASIMR propulsion technology in future space missions.

TABLE OF CONTENTS

CHAPTER

LIST OF FIGURES

Figure

Nomenclature

a_{Earth}	Earth aphelion
a_{Mars}	Mars aphelion
e_{Eart}	Eccentricity of Earth orbit about the sun
e_{Mars}	Eccentricity of Mars orbit about the sun
$e_{s/c}$	Eccentricity of spacecraft orbit about Earth
e_{trans}	Eccentricity of spacecraft transfer ellipse
G	Gravitational constant
g	Earth gravity constant
h	Specific angular momentum
I_{sp}	Specific impulse
$\dot{m}$	Mass flow rate
M_{Earth}	Mass of Earth
M_{Mars}	Mass of Mars
$M_{s/c}$	Mass of the Sun
M_{Sun}	Mass of the spacecraft
P_1	Planet 1: Earth
P_2	Planet 2: Mars
p_x	x-component of position of Spacecraft relative to Earth
p_y	y-component of position of Spacecraft relative to Earth
Q	Spacecraft
R_{Earth}	Radius of Earth
R_{Mars}	Radius of Mars
$R_{s/c}$	Distance measured from center of Earth to spacecraft altitude
r_{Earth}	Earth semi major axis
r_{Mars}	Mars semi major axis
$r_{s/c}$	Spacecraft semi major axis
S	Sun

T	Thrust output of VASIMR engine
t_{Burn}	Burn time for VASIMR engine during departure maneuver
v_x	x-component of velocity of Spacecraft relative to Earth
v_y	y-component of velocity of Spacecraft relative to Earth
v_{Earth}	Orbital velocity of Earth
v_{Mars}	Orbital velocity of Mars
$v_{s/c}$	Orbital velocity of spacecraft about Earth
x	X-component of spacecraft position relative to Earth
$\dot{x}$	First time derivative of x-component of position for spacecraft
$\ddot{x}$	Second time derivative of x-component of position for spacecraft
y	Y-component of spacecraft position relative to Earth
$\dot{y}$	First time derivative of y-component of position for spacecraft
$\ddot{y}$	Second time derivative of y-component of position for spacecraft
θ	True Anomaly
θ_Δ	Phase angle shift
τ_{Earth}	Orbital period of Earth about the sun
τ_{Mars}	Orbital period of Mars about the sun
$\tau_{s/c}$	Orbital period of spacecraft transfer ellipse about the sun
ω_{Earth}	Angular velocity of Earth about the sun
ω_{Mars}	Angular velocity of Mars about the sun

CHAPTER 1
INTRODUCTION

Humanity's desire to reach for the stars has been around since the beginning. Whether it be through the varied stories that hundreds of cultures throughout time have told to describe the sun, moon, and stars or through astronomical curiosity that erupted when Galileo first looked up at the night sky through a telescope; people on this planet have always been fascinated by what stretches out above us. Curiosity began to blossom but no century saw more curiosity simultaneously satisfied and born than the 20th century. Advancements from some of the most horrific conflicts in human history provided the seeds that would allow humanity to grow and reach for the stars. The launch of Sputnik in 1957 began what has become known as the space race and saw the birth of a technological evolution no one could have foreseen. In 1961 Yuri Gagarin would be the first to reach space, even if only momentarily, as he left the Earth's atmosphere. The next year John Glenn would be the first to orbit the Earth and just 3 years after him in 1965 Alexey Leonov would be the first to leave his vessel and take a stroll in space. Reaching for the stars was becoming more than just a motivational metaphor and its relation as a figure of speech officially died in 1969 when Neil Armstrong and Buzz Aldrin became the first human beings to set foot on the moon. In just over 10 years' humanity had gone from looking up at the night stars in awe and wonder to walking amongst the celestial bodies that floated in the dark body of water we called outer space. Unfortunately, that would prove to be the height of public interest and significant achievement for quite some time.

We had reached the moon so fast that everyone expected mars to be right around the corner but sadly that was not the case. 1976 saw the landing of the Viking I and II spacecraft but the achievement did not have the climactic feel that was evident in 1969. The vastness and dangers of space began to fall back into reality and interest began to fade. Even now, almost 40 years in the future, advancements in interplanetary travel have been limited to the landing exploratory robotic spacecraft on mars. Although science fiction would lead people to believe that interplanetary travel should have become more than just fantasy by now; the dangers of space are very real and the problems that have been presented have been very difficult to answer. Aside from the obvious technological and economic issues such as materials, design and assembly,

fuel, and overall mission cost; the most pressing of all are the distance and time estimated for travel.

1.1 Previous Work

The current NASA InSight mission, with submission MarCO onboard, that has been postponed over 2 years from its scheduled lift off in May 2016 after some technical issues arose [18]. The extensive postponement is due to closing of the optimal Earth-Mars trans orbital geometry window that is ideal for NASA to launch such a mission [18]. The absence of a viable and efficient; both technologically and financially, interplanetary propulsion system reduces the means by which missions to Mars are achieved to mere orbital mechanics, where timing and gravity determine when and if missions are launched. VASIMR aims to break those limitations.

The principles behind VASIMR, or Variable Specific Impulse Plasma Rocket, were proposed originally by Dr. Franklin Chang Diaz in 1979 while conducting post-doctorate research in applied plasma physics and fusion technology at MIT. The overall concept behind the new propulsion system was based on the magnetic confinement and propulsion of ionized plasma [12]. Although extensive research and testing would be carried out in the 1980's, the actual breakthrough that would eventually become the VASIMR engine would not occur until 1998 [12]. In 2005 Dr. Chang Diaz founded the Ad Astra Rocket Company whose foundation was based solely on the VASIMR and its potential application to future deep space missions. Although the VASIMR engine system testing is still somewhat in its infancy as research and development of the technology continues; there have been milestones reached as the propulsion system is constantly pursuing perfection.

Early research was dedicated to the initial ionization of the gas propellant in a tube surrounded by to large electromagnetic (RF) wave generators [12]. The magnetic field generated would cause the suspended gas particles to rotate perpendicular to the center of the tube and prevent the plasma from coming into contact with the surface [9]. This would prevent the high temperature plasma from damaging the containment tube leading to system failure and perhaps even leaks in the containment apparatus [9]. It became clear early on that two separate compartments would be necessary in order to successfully ionize the gas to such a degree that propulsion could be achieved [12]. The first compartment is where the neutral gas propellant

would be injected and the first RF generator would emit its helical waves [10]. The purpose of these helical waves is to excite an electron in the gas essentially freeing it creating a positively charged gas particle which once an abundance is generated it shall become plasma [20]. This process continues until the plasma reaches and approximate temperature of 5,800°k at which point the magnetically charged plasma flows into the second chamber [7]. The second compartment uses Ion Cyclotron Heating which is the use of RF waves to accelerate the electrons in the charged gas particles in order to increase kinetic energy and consequently raise the temperature [20]. Once the temperature in the second chamber approaches 10,000,000°k the accelerated ions of the plasma are then convert to linear kinetic energy through a magnetic nozzle that attracts the ions outward at a velocity near 180,000 km/hr [7].

Unfortunately, even at its highest efficiency the thrust to weight ratio generated by the VASIMR engine system, as seen below in figure [A], is still less than 1 [2].

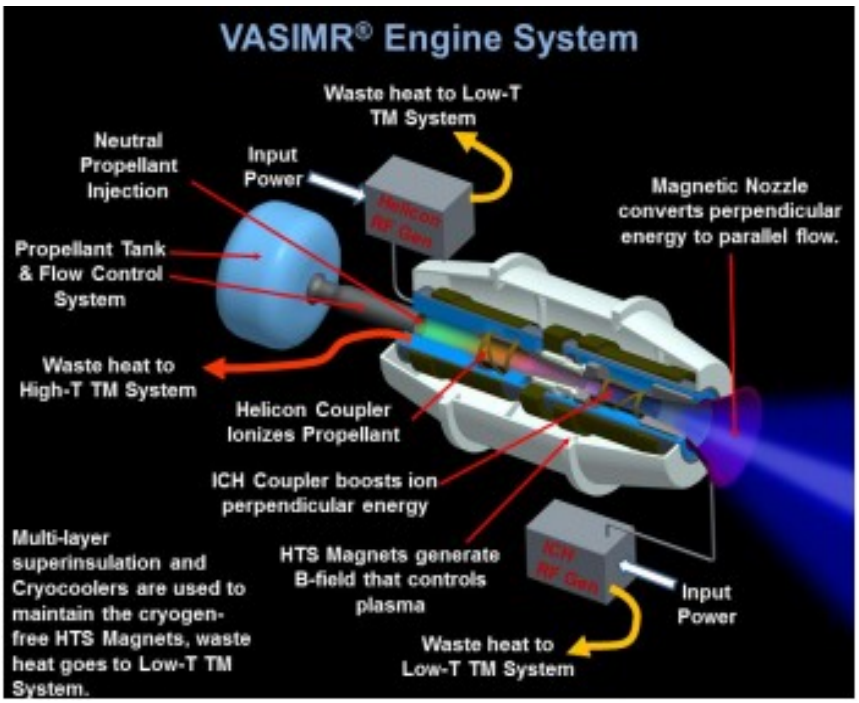

Figure 1.1: Schematic Diagram of a VASIMR SYSTEM [4]

Fortunately, in a Zero-G environment thrust to weight ratios are thought of more in terms of acceleration rather than efficiency [5]. In order to offset such a low thrust to weight ratio; aspects such as specific impulse, measured from 3,000 to 5,000 seconds at max thrust [4], are magnified

to show the extensive lifespan of the VASIMR engine system as seen in figure [B]. Also another interesting capability of the VASIMR propulsion system is the ability to control the generated thrust output allowing for even longer specific impulse times, upwards of 12,000 seconds [1]. Although dwarfed in thrust output when compared to conventional chemical propellants, the specific impulse and shear ability to manually control the thrust output are characteristics no other propulsion system currently possesses [1].

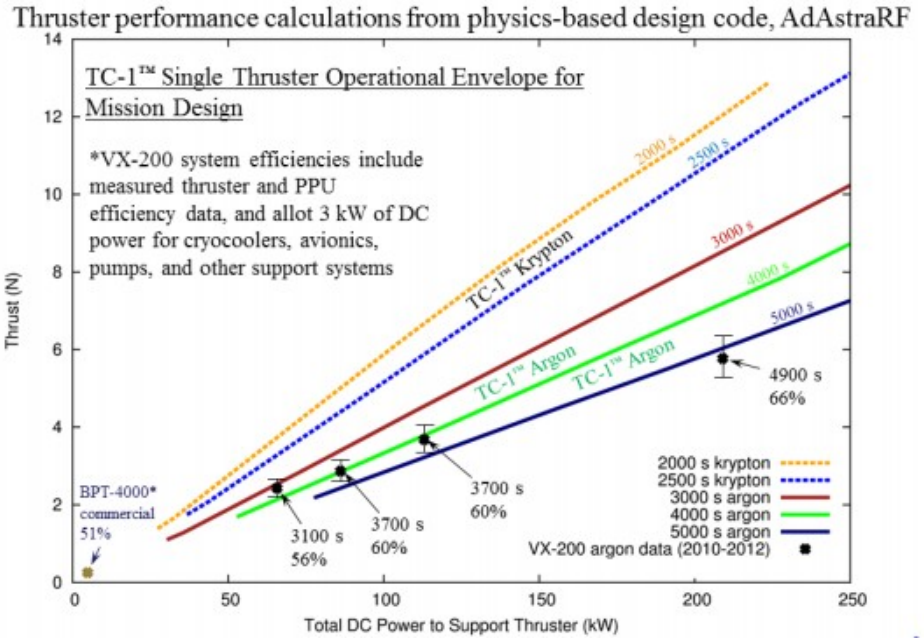

Figure 1.2: System Performance Curves for Argon and Krypton [2]

Presenting testing and calculations both in the research and development as well as in published paper, project the use of either Argon or Krypton as the main fuel source [2] These gases allow for the best efficiencies, around approximately 60% [1], while also being lightweight and presently abundant for testing [22]. There is an issue in regards to refueling but that is a concept that is not even yet in massive consideration as general research and testing are the present focus at this point in time [22].

One of the larger obstacles facing the VASIMR engine system is its need for constant power. Conventional chemical propelled spacecraft and small spacecraft propelled by compressed gas do not a constant source of power to maintain functionality. Through the implementation of a solar grid sufficient power can be generated [2] but structural design will be greatly influenced.

If a hypothetical nuclear reactor power system were integrated, such as the one in figure 1.3, spacecraft structure will not be as impacted and constant steady power can be supplied regardless of solar location. This high energy output system could consistently power multiple VASIMR engines without the need to recharge as solar cells would.

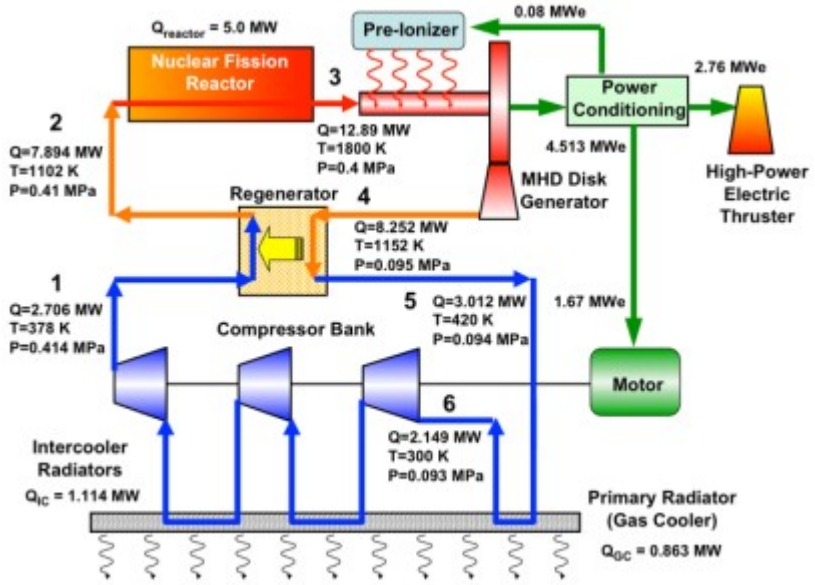

Figure 1.3: General architecture of a nuclear, multi-MW MHD-VASIMR sys. [5]

Current space flight for the most part has consisted of large propellant burns combined with orbital mechanics in order to achieve mission objectives. However, for interplanetary travel constant propulsion is required to decrease the space flight times [8]. With a nuclear power source, electric propulsion systems could be throttled for vast amounts time allowing for extensive, varied if desired, acceleration periods [8]. This would also for solar electric propulsion systems to be included purely as a redundancy measure should the nuclear power source experience any malfunctions [22].

As stated in section 1.1 the current projected Earth to Mars space flight time is projected to last at minimum 6 months which coincidently was the projected duration for a round trip mission in a Nuclear Electric Powered (NEP) VASIMR spacecraft as seen in figure 1.4.

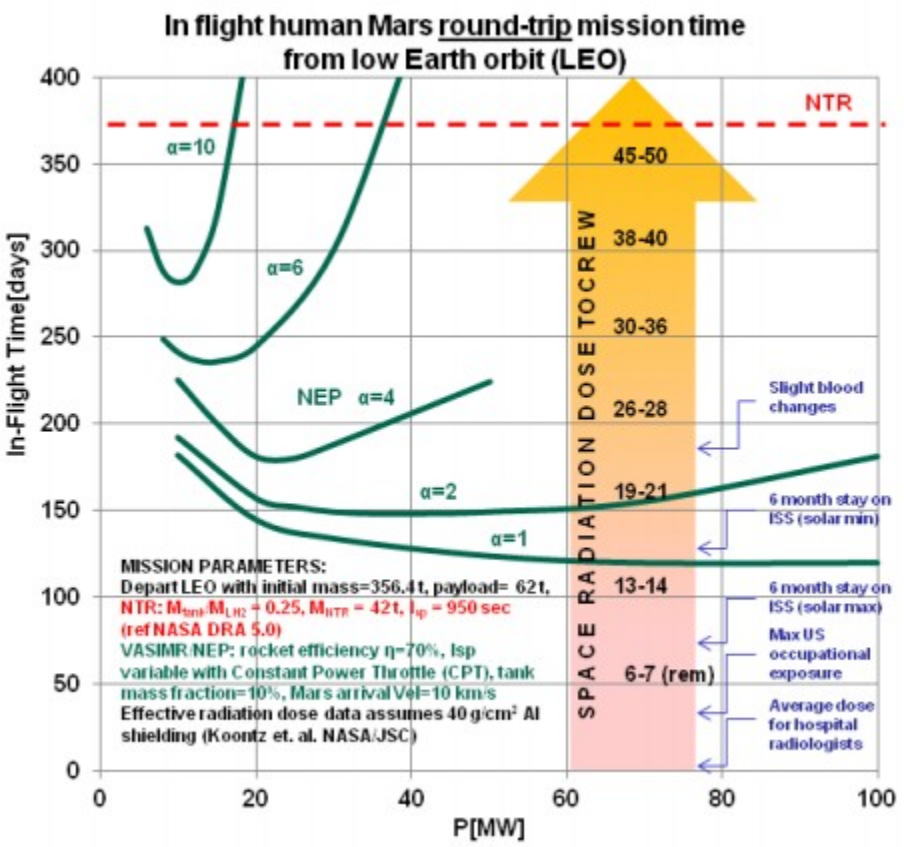

Figure 1.4: Radiation exposure against in-flight duration vs power required for VASIMR human Mars Mission [5]

The exposure to radiation is the key concern for human interplanetary travel to Mars which stems from the length of the mission. Figure 1.4 was determined using the current VX-200 prototype as opposed to the earlier prototypes VX-100 and VX-50, the numbers which correspond to required energy input in kilowatts [5]. It is this extreme exposure to solar radiation that is presently the largest obstacle for human missions that will cover vast distances [15]. Unfortunately, figure 1.4 also illustrates the fact that transportation of manned spacecraft will require high mass vehicles and hence require amounts of energy, to the order of Megawatts, that solar electric propulsion simply cannot produce at this moment [22]. The vast amount of energy will be needed to power the VASIMR propulsion system, avionics, living quarters, exercise area, kitchen and food storage, communications, and many other systems essential for the astronauts to maintain adequate health for months as long term exposure to zero gravity and abnormal sleep patterns can cause substantial psychological and physiological health issues [14]. Cardiovascular

problems and muscular atrophy can develop without exposure to Earth's gravity as well as dementia and depression [14]. Nuclear electric propulsion must progress in a similar fashion as the VASIMR engine if the idea of manned interplanetary flight is to come to fruition otherwise humans will not see the end of the mission.

The aim of this paper is to present astrodynamics calculations and a 3-dimensional simulations for various configurations of a practical application of the VASIMR engine for a purely theoretical unmanned mission to Mars. The primary function of this hypothetical spacecraft will be to traverse the distance from Earth to Mars in the fastest time as possible. The broad aspects of the hypothetical spacecraft will be based on the present InSight and MarCo Mars missions in terms of mass, deployment window, and payload with added mass for the VASIMR engine and its operational systems under the current 3kg/kw [22] weight-to-power ratio. For the purpose of this project it will be assumed that the power subsystem will provide sufficient energy for the VASIMR engine as well as any other onboard subsystems. The calculations will be compared to widely recognized Hohmann Transfer scenario in order to properly demonstrate efficiency and viability.

This paper is also to demonstrate the effects of a VASIMR engine on interplanetary travel while highlighting the efficiency in travel time as well as promoting the wide acceptance of electric powered plasma propulsion is the main focus for future propulsion technological focus. Chapter 2 will outline the methodology and mathematical approaches for both the Hohmann Transfer scenario, as well as the varying Configurations for the VASIMR spacecraft. Chapter 3 will serve as an overview in regards to the setup in Matlab and how the order of the programs will be organized chronologically to demonstrate the base Homann Transfer scenario, the VASIMR scenario with the ability to adjust accordingly for various scenarios and lastly the Simulink code which will generate the 3-dimensional simulation. Chapter 4 will establish all assumptions and initial conditions that allow for the astrodynamics calculations to be carried out and allow for translation of that data into the simulations. Chapter 5 will demonstrate the calculated values, graphs showing trajectories, and time lapsed snapshots of the simulations to visually demonstrate the results. And chapter 6 summarize all conclusions as well as give further details into present work and future plans for VASIMR at the AdAstra Rocket Company in Houston Texas.

CHAPTER 2
METHODOLOGY AND MATHEMATICAL APPROACH

In order to provide this project with validity, the widely recognized Hohmann transfer scenario will be used as a base for comparison with the VASIMR engine scenarios. The approaches and equations discussed and shared in this chapter all come from (Hunter 2016) and (Curtis 2013). The first part of the project will deal with the various aspects that comprise the Hohmann transfer maneuver as well as graphical depictions of the resulting orbits. The second part of the project will establish a base model for a spacecraft equipped with a standard 2x200 kilowatt VASIMR engine configuration with the ability to adjust accordingly for scenarios with various engines.

2.1 Hohmann Transfer Approach

Although both share some similarities in equations and methodology, the Hohmann Transfer scenario is based solely upon a single thrust maneuver that greatly increases velocity for a small amount of time. We begin by calculating the orbital velocities, using equation 2.1 of the spacecraft about its starting point and its destination, which in this case will be Earth and Mars respectively.

$$V_{circ} = \sqrt{\frac{G * M_{pt}}{r_P}} \tag{2.1}$$

The maneuver then begins from equation 2.2 below which gives us the velocity the spacecraft will have once it enters the transfer ellipse.

$$P_{1V^Q} = \Delta V_1 = v_\infty = \sqrt{\frac{G M_{sun}}{r_1}} * \left(\sqrt{\frac{2 * r_2}{(r_1 + r_2)}} - 1 \right) \tag{2.2}$$

Next we must determine the velocity burst necessary to escape Earth's Sphere of Influence (SOI) This allows the spacecraft to shift its orbit to a transfer ellipse at a velocity determined by equation 2.3 below:

$$necessary\ \Delta V = V_P - V_\circ = \sqrt{v_\infty^2 + \frac{2*G*M_p}{r_P}} - \sqrt{\frac{G*M_p}{r_P}} \qquad (2.3)$$

As the burst from the engine creates a change in the eccentricity of the spacecraft orbit. The new transfer ellipse now crosses paths with the intended target object orbit as seen below in figure 2.1

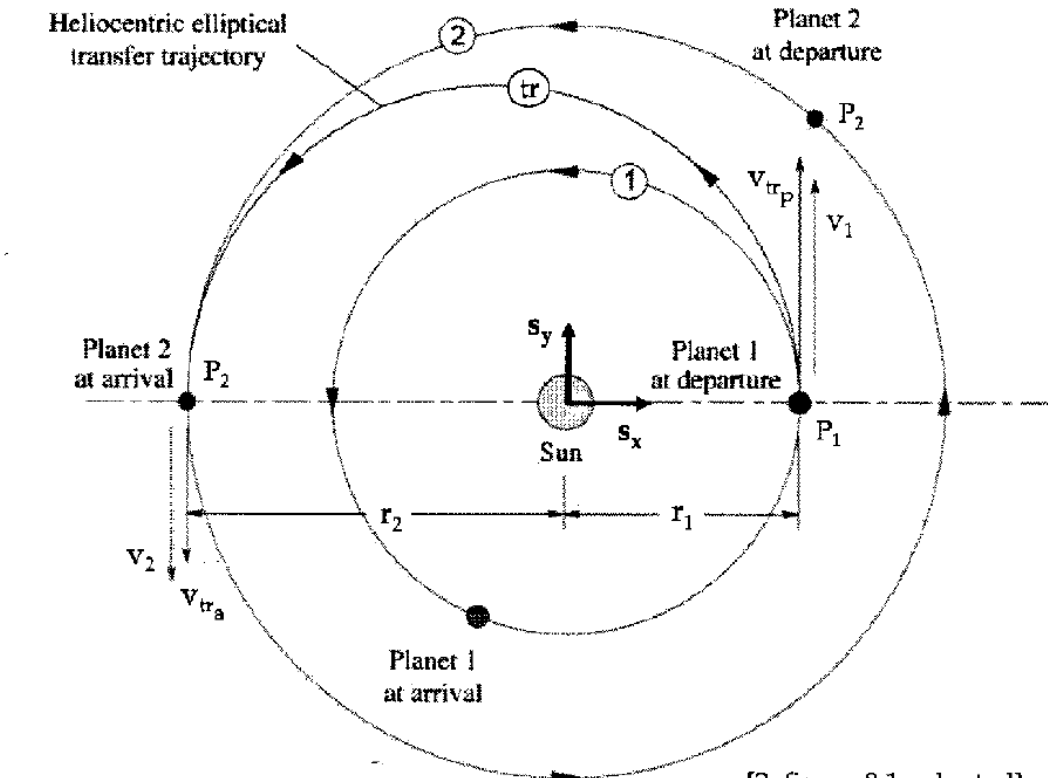

Figure 2.1: Depiction of Ideal Hohmann Transfer Scenario between two circular orbits

Now the process is somewhat reversed as we calculate the approach velocity of the spacecraft relative to the 2nd planet using equation 2.3:

$$P_{2V^{Q}} = \Delta V_2 = v_{\infty_2} = \sqrt{\frac{G M_{sun}}{r_2}} * \left(1 - \sqrt{\frac{2 * r_1}{\left(r_1 + r_2\right)}}\right) \tag{2.4}$$

Lastly we must now calculate the velocity burst maneuver that will slow the spacecraft down just enough to fall into a circular orbit about the planet by using equation 2.2 again but in a slightly different fashion. This time the maneuver is negative as the spacecraft will be settling into an orbit rather than trying to escape. All orbits can be calculated, including the path of the transfer ellipse, using equation 2.5:

$$r_P = \left(\frac{a * \left(1 - e^2\right)}{1 + e}\right) \tag{2.5}$$

just by simply inserting the respective aphelion and eccentricities. From the orbits we can determine intersection followed the necessary phase angle shift after the period below

$$\tau = 2 * \pi * \sqrt{\frac{a_p^3}{G * M_p}} \tag{2.6}$$

is determined then difference in π orbit revolutions determines the amount of time taken for the entire mission.

2.2 Continued Burn Approach with VASIMR Engine

For the continuous burn approach, the position, velocity, and acceleration of the spacecraft now become functions of 1st and 2nd order differential equations in each direction as seen in equations 2.7, 2.8, and 2.9.

$$\acute{x} = \frac{-GM}{r^3} x + \frac{T}{m}\left(\frac{\acute{x}}{v}\right) \tag{2.7}$$

$$\acute{y} = \frac{-GM}{r^3} y + \frac{T}{m}\left(\frac{\acute{y}}{v}\right) \tag{2.8}$$

$$\dot{z} = \frac{-GM}{r^3} z + \frac{T}{m}\left(\frac{\dot{z}}{v}\right) \tag{2.9}$$

Although thrust will be constant throughout the burn, the velocity, position, and mass will also become time dependent equations with the radius being a vector function as well. Mass can be easily calculated as seen in equation 2.10:

$$M(t) = M_{s/c} + (\dot{m} * t_{burn}(t)) \tag{2.10}$$

with

$$\dot{m} = \frac{T}{I_{sp} * g} \tag{2.11}$$

The radius on the other hand will be a bit more difficult as the position vector must be broken up into components at each time interval and added to the next interval before the magnitude can be taken again. This leads the initial calculation of the equations 2.7-2.9 at $t_{Burn} = 1$ and being integrated into equations 2.12 and 2.13 below:

$$v_n(t) = v_n(t_{Burn} - 1) + \dot{x}(t_{Burn}) \tag{2.12}$$

$$p_n(t) = p_n(t_{Burn} - 1) + \dot{x}(t_{Burn}) \tag{2.13}$$

Where n represents the axis frame, x or y-axis, and magnitude is calculated from the 3 axis components for each time interval but the z-axis is held steady at zero due to the 0° inclination assumption. This process is repeated until t reaches the end of t_{Burn} which is approximately 15, or 900 seconds. Similarly, the specific angular momentum and eccentricity vectors as well as the true anomaly are also functions of the time differential and must be calculated at each time interval but only after the velocity and position vectors have been calculated.

$$\vec{h}(t) = (\vec{p}(t) \times \vec{v}(t)) \tag{2.14}$$

$$\vec{e}(t) = \frac{(\vec{v}(t) \times \vec{h}(t))}{G * M_{Earth}} - \frac{\vec{p}_n(t)}{\|\vec{p}(t)\|} \tag{2.15}$$

$$\theta(t)=\cos^{-1}\left(\frac{\vec{p}_n(t)\cdot\vec{e}_n(t)}{¿¿\left\|\vec{p}(t)\right\|*\left\|\vec{e}(t)\right\|}\right) \tag{2.16}$$

then simply just graph true anomaly at its respected time interval to generate the graphs of motion as the continuous burn occurs.

CHAPTER 3

PROGRAM AND SIMULATION SETUP

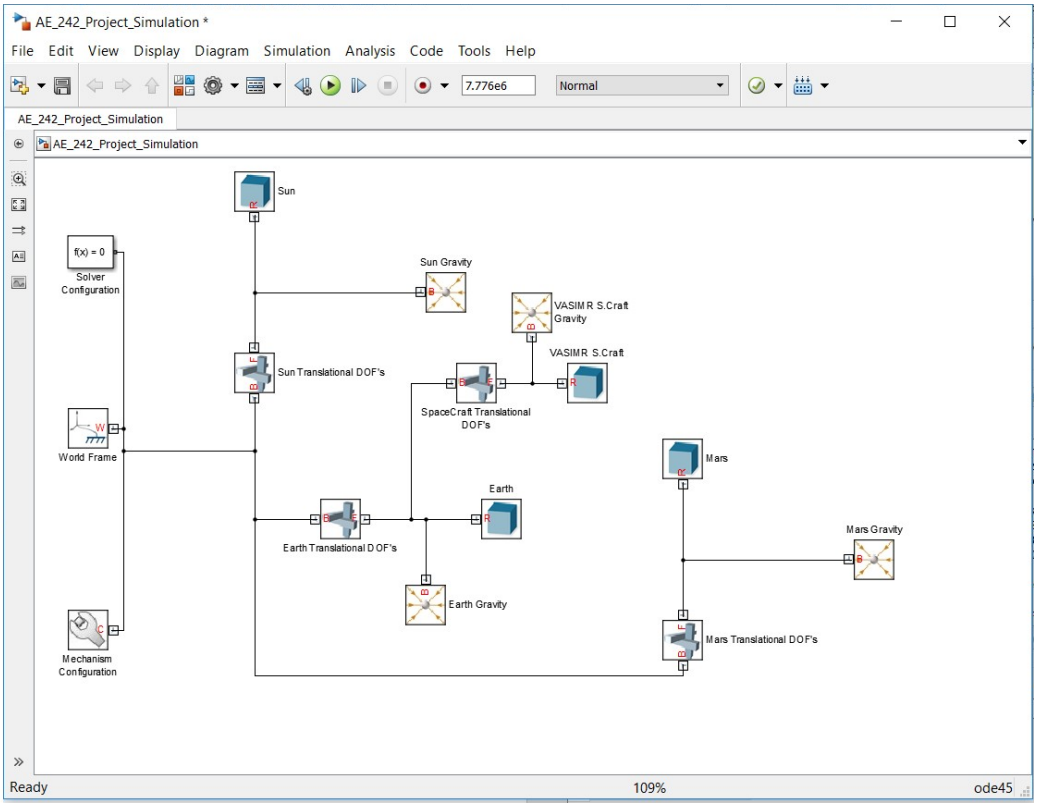

Figure 3.1: Simulink model for generating 3-D astrodynamics simulation

The Matlab code will be separated into two large m-files; one for the base Hohmann Transfer scenario and the other will serve as the model for VASIMR engine configurations. Figure 3.1 represents the Simulink layout that will generate the 3-dimensional simulations. That file will also have its own Matlab code subroutines that can be altered to account for various engine configurations and phase angle shifts in Mars orbit as the period of the transfer ellipse decreases with a larger thrust burn.

It is important to note that these programs and simulations were run on the publicly accessible student version that can be purchased from the Mathworks website. The student version was used due to its financial benefit as well as the added benefit of ease of access.

CHAPTER 4

INITIAL CONDITIONS, ASSUMPTIONS, AND VARIOUS SCENARIOS

Interplanetary planetary travel is incredibly complex and full of unknown variables that make the calculation of risk tremendously difficult. There are so many factors that can affect the transition of a spacecraft from orbiting one planet to another. Dangers and perturbations to interplanetary calculations can stem from solar radiation, solar winds, gravitational forces due to the sun and other planets, solar flares, any errors in spacecraft systems, and small asteroids. However, for simplification purposes in this project, calculations will be completed under the assumption that any risk from floating space debris will be nonexistent. Also perturbations due to any of the factors aforementioned or not listed will be neglected along with any corrections that may have to be accounted for in terms of changing spacecraft mass due to propellant use. Also it will be assumed that Earth, Mars, the Sun, and the Spacecraft will be located on the same plane of reference. Any discrepancies in orbit plane inclination will be assumed to be negligible allowing for a benchmark comparison as the level of computing power for those calculations and 3-D simulations is not easily accessible. Some of the global constants are listed below:

Planet	*Mass (kg)*	*Radius (km)*	*Semi-Major (km)*	*Aphelion (km)*	*Perihelion (km)*	*eccentricity*	*Period (days)*
Earth	*5.972e24*	*6378*	*149,600,000*	*152.1*	*147.1*	*.0167*	*365.2*
Mars	*6.4171e23*	*3390*	*227,920,000*	*249.2*	*206.6*	*.0935*	*687.0*
Sun	*1.989e30*	*695,800*	*0*	*0*	*0*	*0*	*0*

The project spacecraft will be treated as a particle moving about the relative 2-D plane in which the celestial bodies are located and its mass will be 6000kg. This is based upon the InSight and MarCo missions with added mass to account for the weight-to-power ratio of the various engine configurations as well as spare mass for other components and subsystems. Propulsive forces exerted by the spacecraft will vary as the use of propulsion in this project as each configuration will increase the thrust output but burn time and specific impulse will remain constant. Other constants will be used such as the Universal Gravitational Constant G (6.67e-20 $km^3/kg*sec^2$) and Earth's local gravity g (9.81 m/sec^2) will be used throughout this project.

4.1 Various VASIRM Engine Configurations

In terms of the spacecraft, for now it will be hypothetically powered by a purely theoretical nuclear reactor as noted that solar electric propulsion will not produce the necessary power to operate the propulsion system as well as all other mission subsystems. The table below depicts the necessary characteristics for one dual core VASIMR engine.

VASIMR Spacecraft	*Mass (kg)*	*Radius (km)*	*Fuel Type*	*Max Isp (sec)*	*Max Burn Time (sec)*	*Max Power (kw)*	*Max Thrust (N)*
2 Engine Configuration	*6000*	*.01*	*Argon*	*5000*	*900*	*200*	*10.2*
4 Engine Configuration	*“”*	*“”*	*“”*	*“”*	*“”*	*“”*	*20.4*
6 Engine Configuration	*“”*	*“”*	*“”*	*“”*	*“”*	*“”*	*30.6*

There will be 2 other configuration scenarios with 4 and 6 engines integrated into the hypothetical spacecraft. However, due the large initial mass, the added engines and propellant will fit within the proposed spacecraft mass. The burn time, specific impulse, and fuel type will not change in order to maintain consistency when comparing the scenarios. The initial orbit, which is depicted in figure 4.1,

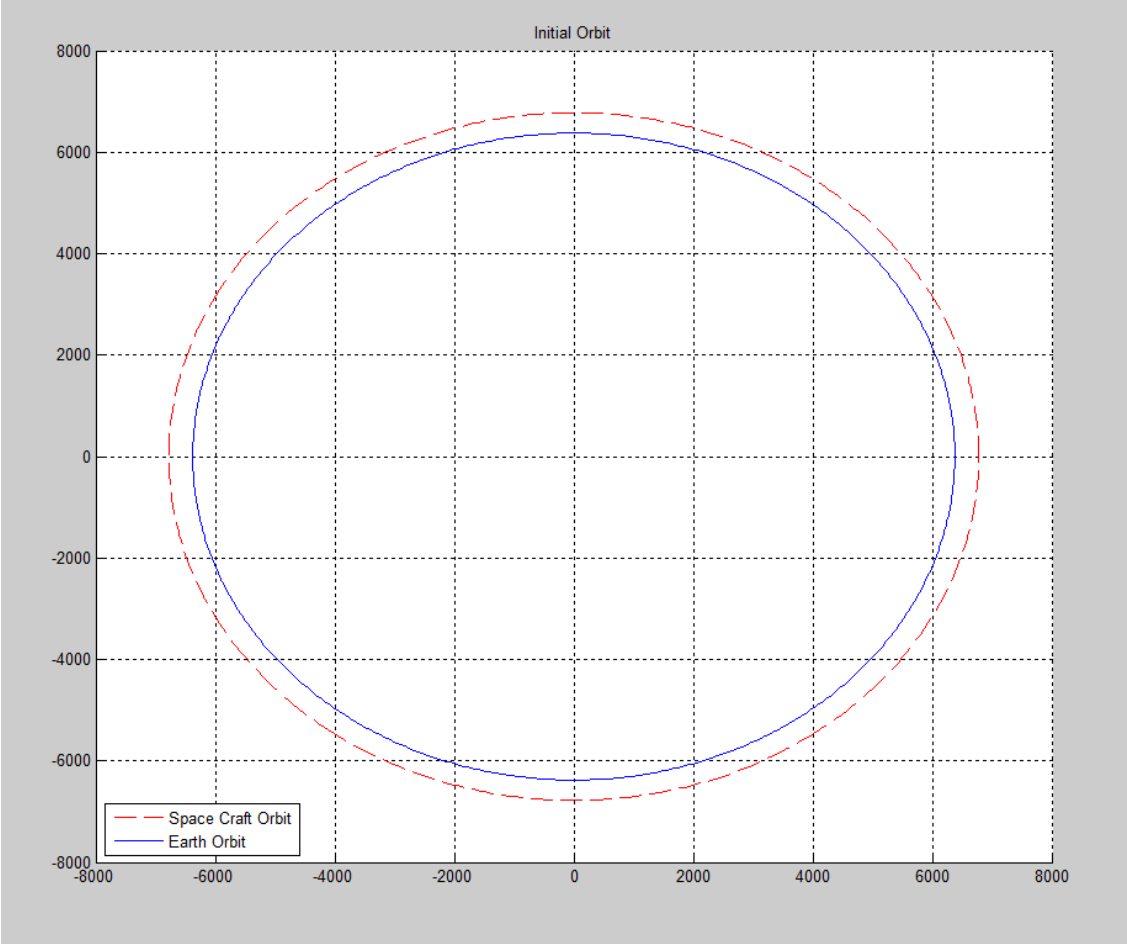

Figure 4.1: Graphical representation of spacecraft initial orbit about Earth

will be at approximately 400km altitude, corresponding to the approximate orbit of the ISS, as it is the implication that any mission utilizing the VASIMR technology will depart from the ISS; treating it as a sort of home base. All calculations and simulations will begin when the spacecraft velocity is perpendicular to the Earth's relative x-axis as depicted previously in figure 2.1. This will allow simpler initial conditions in both the Hohmann transfer and VASIMR engine configuration scenarios. Likewise, Earth's relative position to the sun will be when the Earth is has reached its Aphelion position and its velocity vector will also be perpendicular to the Sun's relative x-axis. Mars' phase shift angle, velocity vector, and initial positon vector will be calculated using equations 2.4 and 2.5; using the spacecraft's calculated eccentricity at departure, combined with trigonometric calculations.

CHAPTER 5

GENERATED GRAPHS AND SIMULATIONS

This section will be separated into 4 parts; The Hohmann Transfer Scenario will be first and serve as the base model and then 3 separate VASIMR engine configurations: 2x200kw, 4x200kw, and 6x200kw, to demonstrate the application and efficiency of multiple VASIMR engines. Each of the 3 configurations will consist of graph depicting spacecraft orbit during acceleration and snapshots of the spacecraft as it travels to Mars

5.1 Hohmann Transfer

The calculations from scenario I have demonstrated that a Delta V of approximately 3.5679 km/sec is required for the spacecraft to escape Earth's gravity and reach Mars in approximately 283.761 days or .77142 years after Mars phase angle shift is applied. This transfer time window is just over 9 months which is around what NASA is currently operating under. The subsequent scenarios will aim to greatly reduce this time required for travel. The transfer ellipse along with the orbits of Earth, Mars, and the initial spacecraft orbit are displayed in figure 5.1 to visually depict the Hohmann Transfer window.

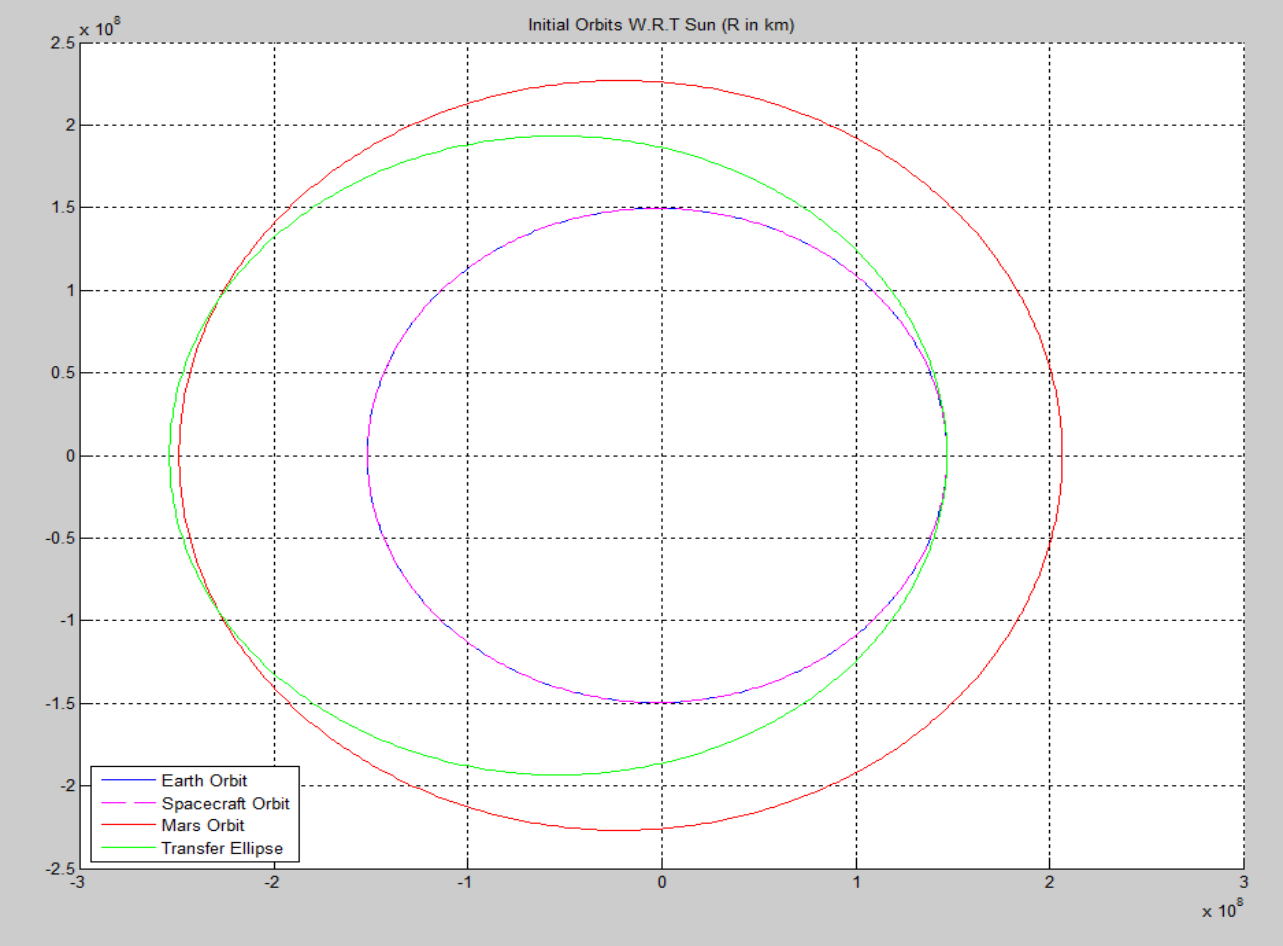

Figure 5.1: Graphical representation of Hohmann Transfer maneuver

The intersections of the transfer ellipse and Mars' orbit are can be clearly seen and confirm the approximate time of travel. Mars phase angle shift is calculated only to assist in time of departure to ensure that when the spacecraft crosses the Mars orbit, Mars is in the same location allowing for a second burn so that the spacecraft can fall into a Mars synchronous orbit. The orbits themselves do not change. The difference in orbital radius between and the spacecraft is approximately 400km, which corresponds to the orbital altitude of the International Space Station (ISS), but this graph shows how miniscule that distance is when compared to other astronomical distances.

5.2 Configuration 1: 2x200kw VASIMR Engine

The Calculations from configuration I are divide into two parts with the first being the carrying out of the constant thrust maneuver and calculating the velocity at the end of the burn. Second being the simulation of the spacecraft as it departs from Earth. Given the characteristics of the VASIMR engine and applying them to the spacecraft it has been calculated that the thrust burn maneuver will allow the spacecraft to achieve a velocity of approximately 8.7544 km/sec after completing approximately 5.5 revolutions as seen in the figure 5.2.

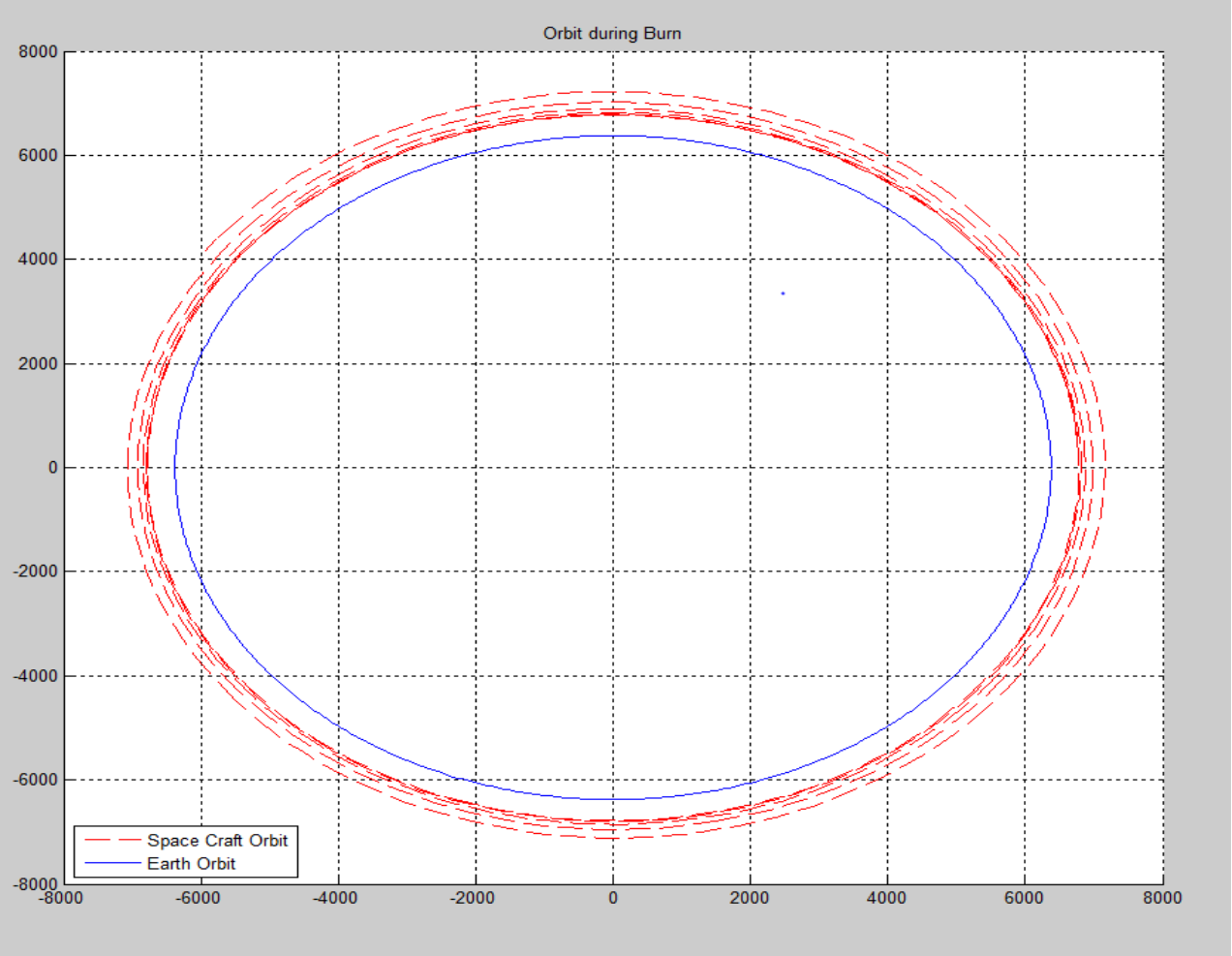

Figure 5.2: Graphical representation of time lapsed VASIMR thrust burn for configuration 1

Once the burn is complete and the velocity has reached its maximum, the resultant velocity vector was then used as the input vector for the 3-D simulation which can be ran in Simulink with the adjusted code in the subroutines. The Simulation depicts a correct

interplanetary trajectory allowing for Mars orbit capture but most impressively is the fact that this is accomplished in approximately .246 years or 90 days. That is an 68% decrease from the current NASA estimates. Snapshots of the simulation at 3 points; initial, approximate middle, and approximate end, are taken to demonstrate the effect of the VASIMR engine continuous burn and the calculated phase angle shift for the reduced transfer time.

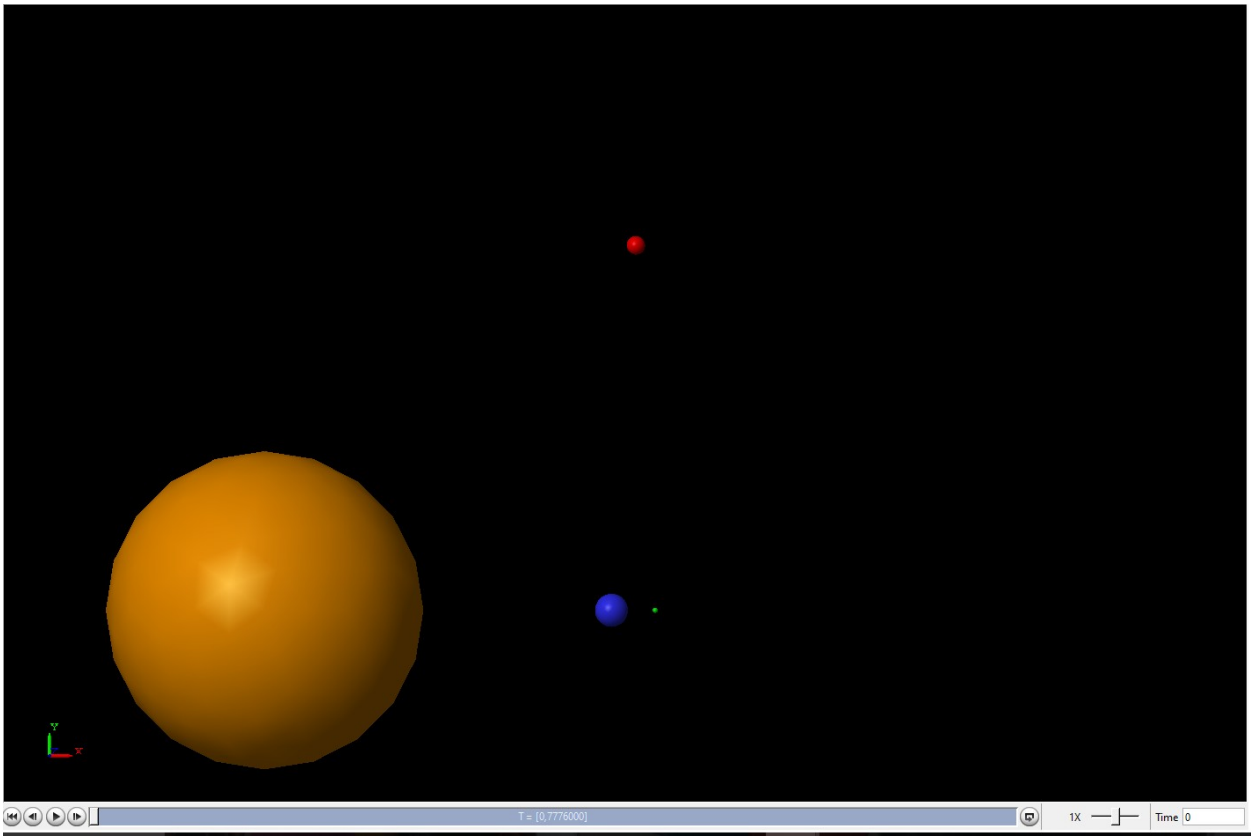

Figure 5.3: Top-view Screenshot of 3-D simulation at t = 0 secs

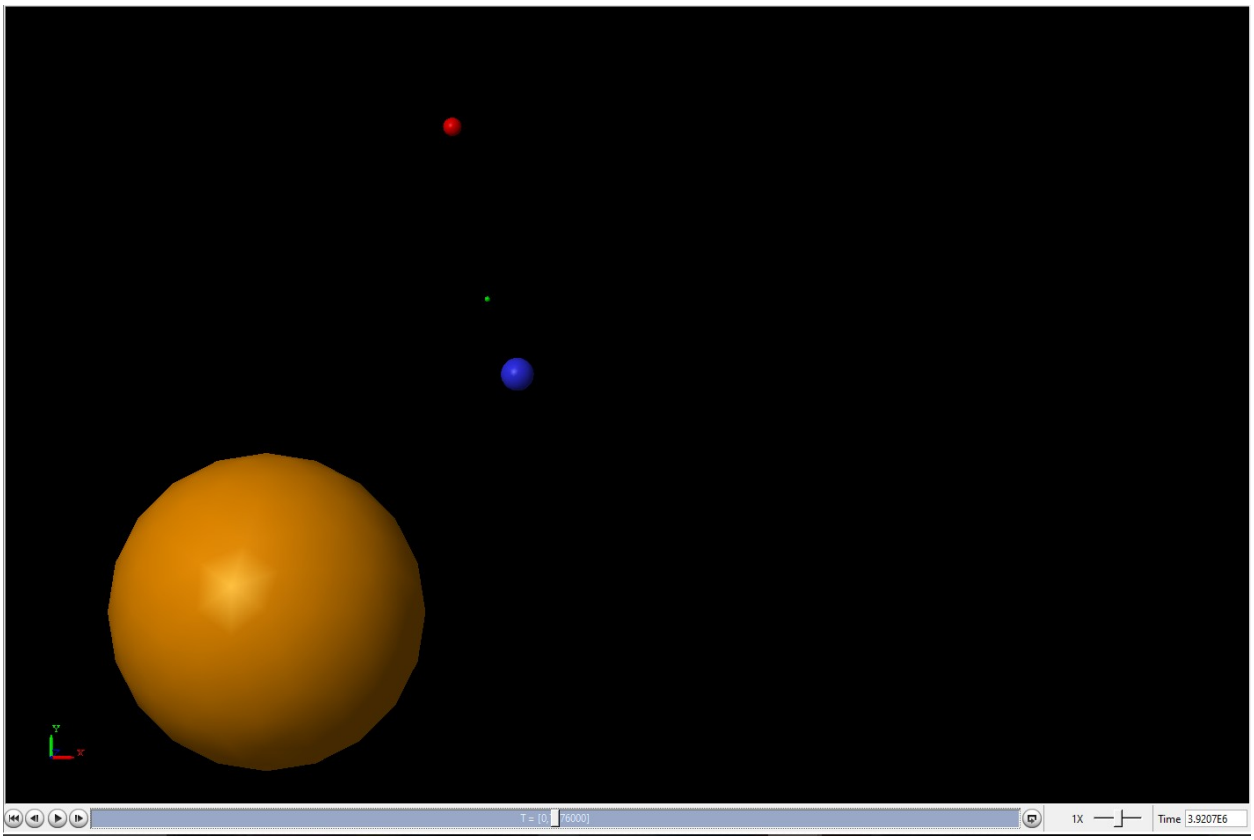

Figure 5.4: Top-view Screenshot of 3-D simulation at t = 3.9207e6 secs or ~ 45 days

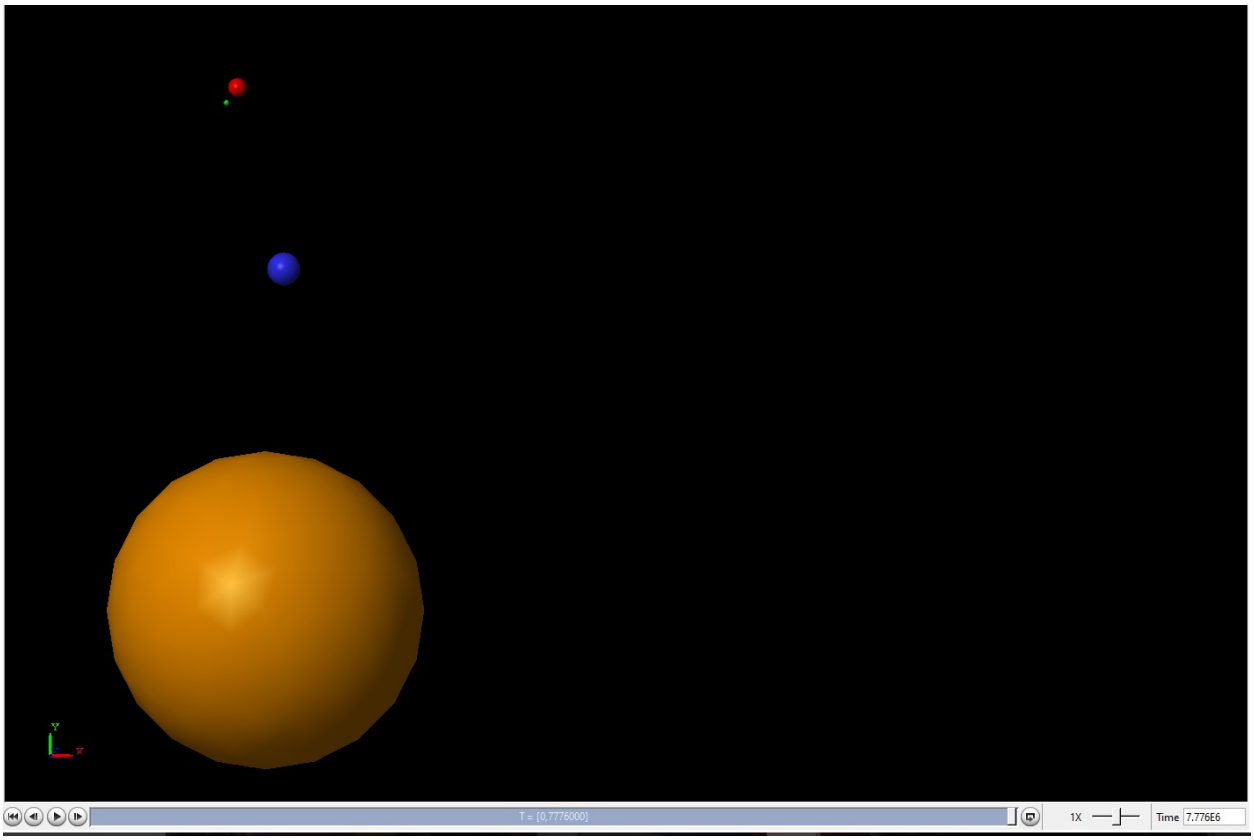

Figure 5.5: Top-view Screenshot of 3-D simulation at t = 7.776e6 secs or ~ 90 days

The visual representations of the Earth, Mars, and the spacecraft have been scaled up for the sake of comparison. This model would not be possible if all planets and spacecraft were to scale. These are all top view image captures as all bodies lie on the same equatorial plane and there are no position, velocity, or acceleration components in the z-directional axis. The time lapses seen in the bottom right hand corner are in seconds and the overall simulation is approximated to last 3 seconds with each passing second accounting for approximately 30 days of travel time. The simulation is terminated when the spacecraft is deemed to approach a sufficient distance so that the subsequent deceleration maneuver can be performed or a flyby course can be initiated.

5.3 Configuration 2: 4x200kw VASIMR Engine

Exactly like configuration I, Calculations from configuration II are divide into the previously stated two parts with the exception of the double the thrust force. For this configuration it has been calculated that the thrust burn maneuver will allow the spacecraft to achieve a velocity of approximately 9.9429 km/sec after completing approximately 6.1 revolutions as seen in the figure 5.6.

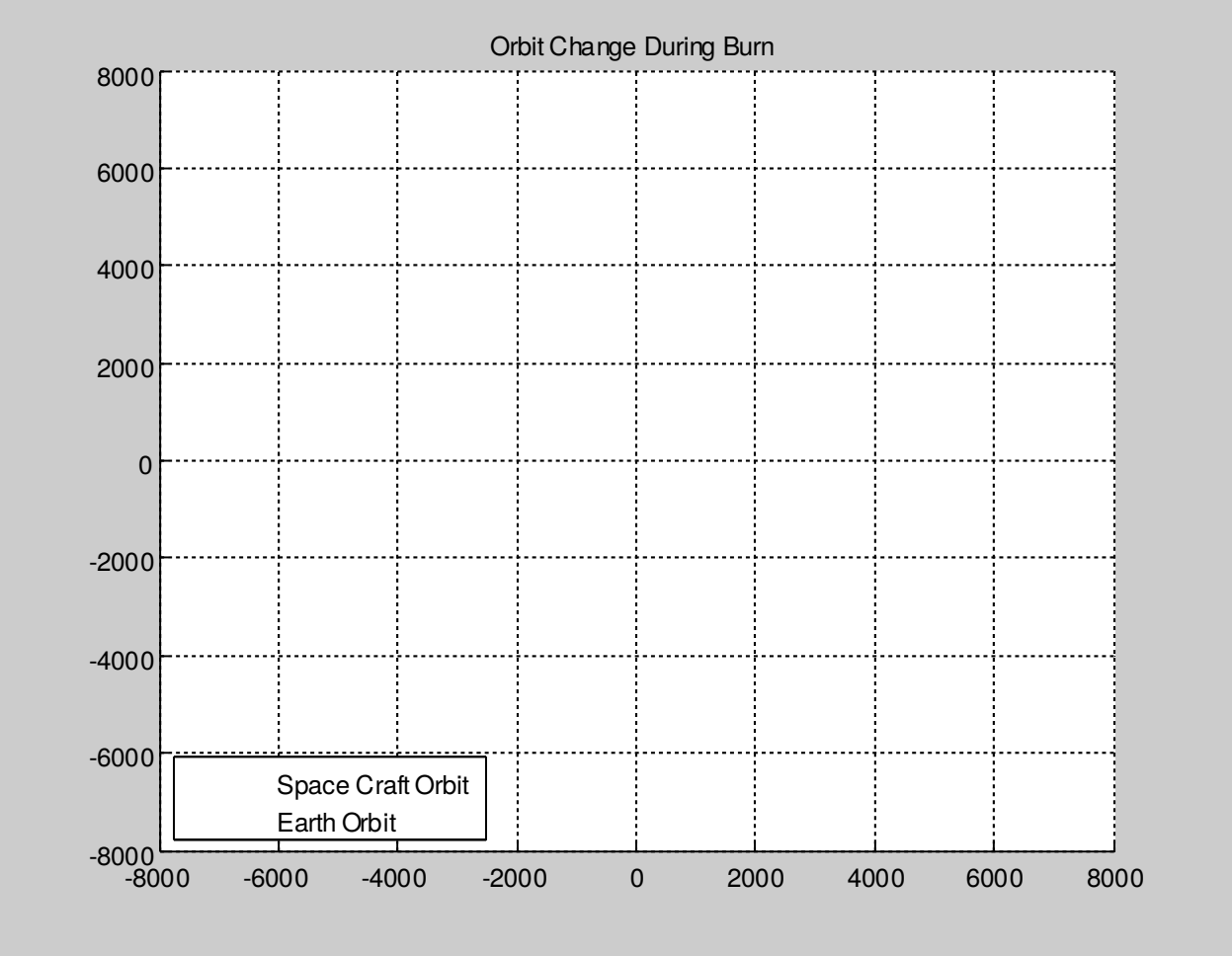

Figure 5.6: Graphical representation of time lapsed VASIMR thrust burn for configuration 2

This configuration clearly demonstrates a decrease in the travel but unfortunately not a significant amount to concluded high efficiency. The Simulation depicts that the interplanetary trajectory is accomplished in approximately .224 years or 82 days. That is only a 9% decrease from scenario I. Snapshots of the simulation at 3 points; initial, approximate middle, and

approximate end, are taken to demonstrate the effect of the VASIMR engine continuous burn. In order to better visually demonstrate any increases in efficiency, in regards to reduced travel time; Earth, Mars, and the spacecraft will begin from the same initial conditions as configuration I.

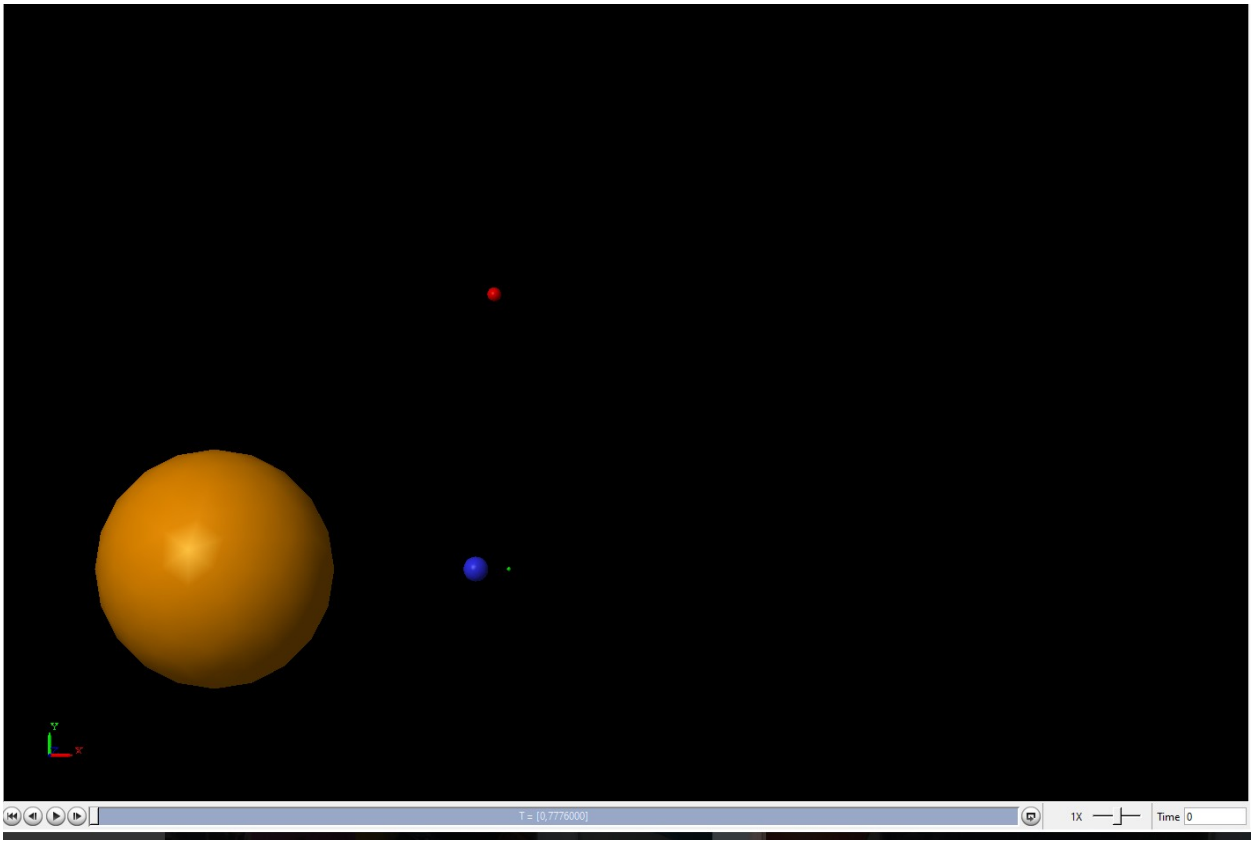

Figure 5.7: Top-view Screenshot of 3-D simulation at t = 0 secs

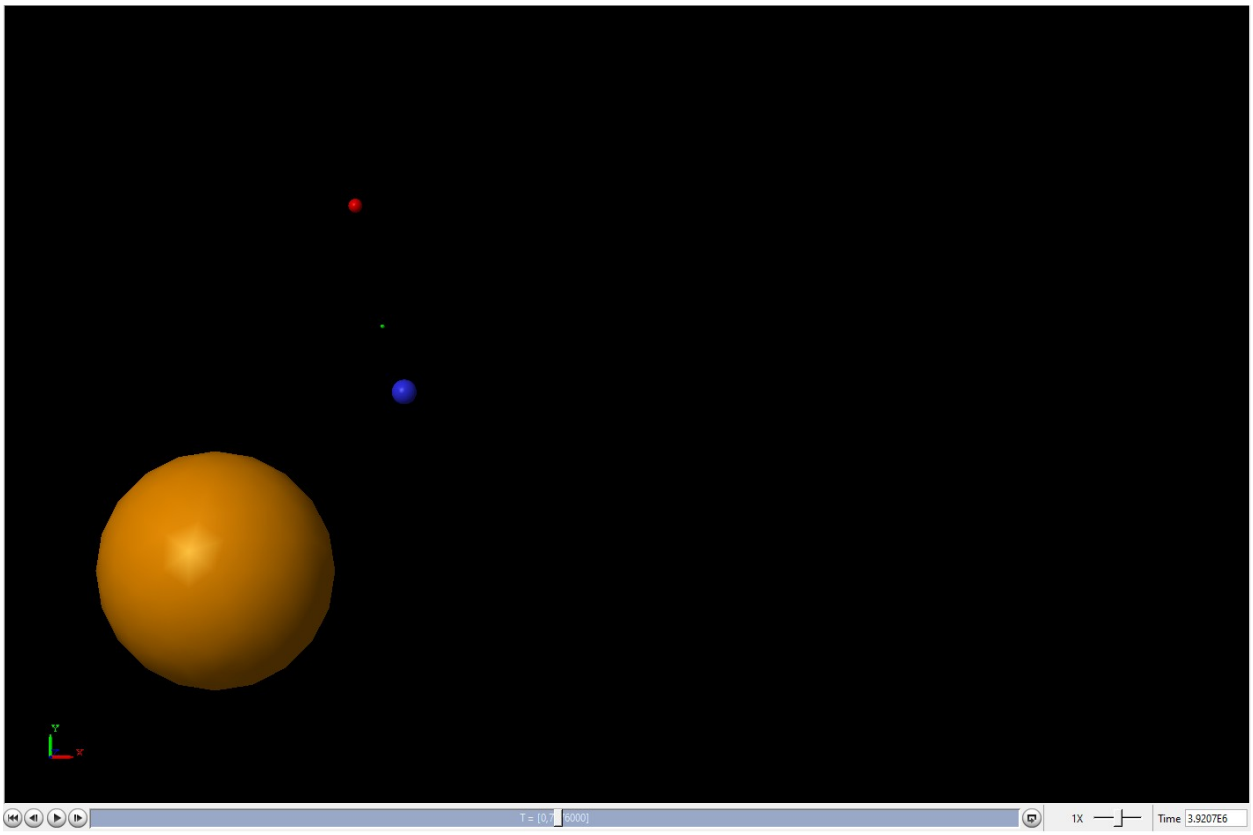

Figure 5.8: Top-view Screenshot of 3-D simulation at t = 3.9207E6 secs or ~ 45 days

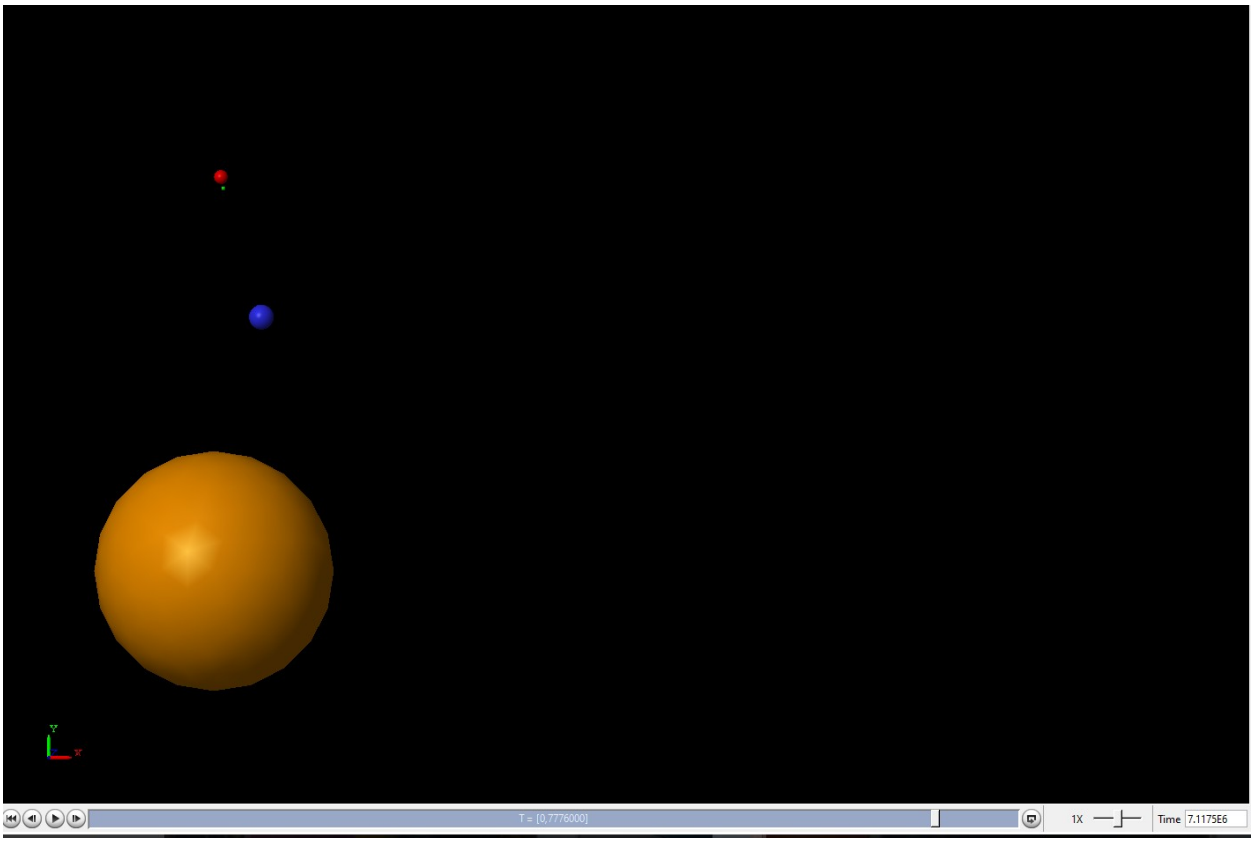

Figure 5.9: Top-view Screenshot of 3-D simulation at t = 7.1175E6 secs or ~ 82 days

The simulation for configuration II shows that the spacecraft intersects with the Mars orbit at an earlier point in the orbit as oppose to configuration I shown in figure 5.5. This configuration appears to be more well suited for a direct insect with the planet if landing on the surface is a key goal of the mission. However, it must also be noted that under the proper Mars phase angle shift, intersect for spacecraft may occur earlier, though perhaps not to a significant degree, and with a more desired orientation.

5.4 Configuration 3: 6x200kw VASIMR Engine

Lastly, calculations from configuration III are divide into the previously stated two parts with the exception of the triple the thrust force. For this configuration it has been calculated that the thrust burn maneuver will allow the spacecraft to achieve a velocity of approximately 11.2157 km/sec after completing approximately 6.7 revolutions as seen in the figure 5.10.

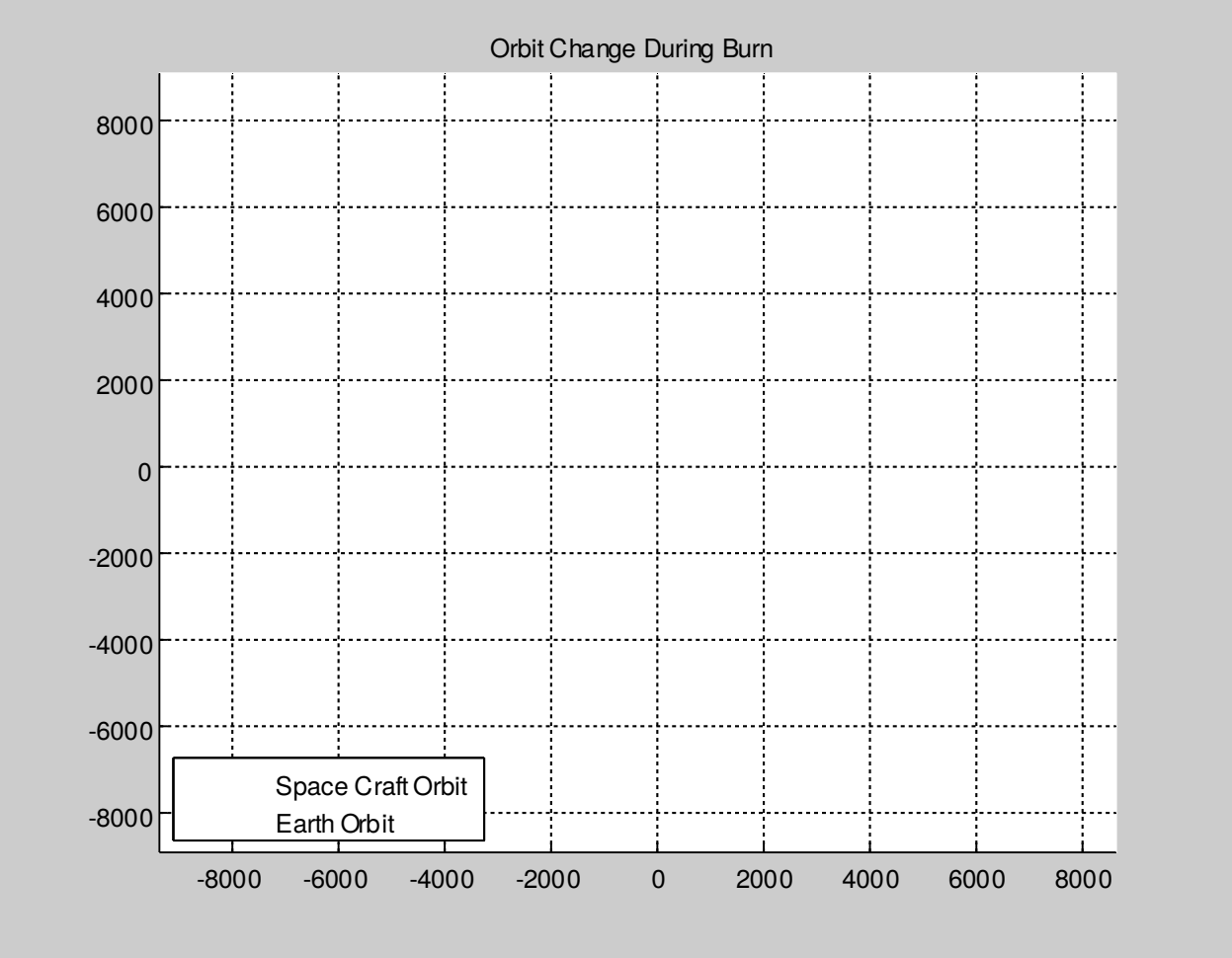

Figure 5.10: Graphical representation of time lapsed VASIMR thrust burn for configuration 3

This configuration also demonstrates a decrease in the travel but unfortunately yet again; not a significant amount to concluded high efficiency. The Simulation depicts that the interplanetary trajectory is accomplished in approximately .213 years or 78 days. That is only a 14% decrease from scenario I and only 5% improvement from configuration II. The snapshots of the simulation at 3 points; initial, approximate middle, and approximate end follow to visually

demonstrate the effect of the VASIMR engine continuous burn. The same initial conditions and velocity and positions vectors are used as well as the sizing scale for all 4 bodies to maintain consistency.

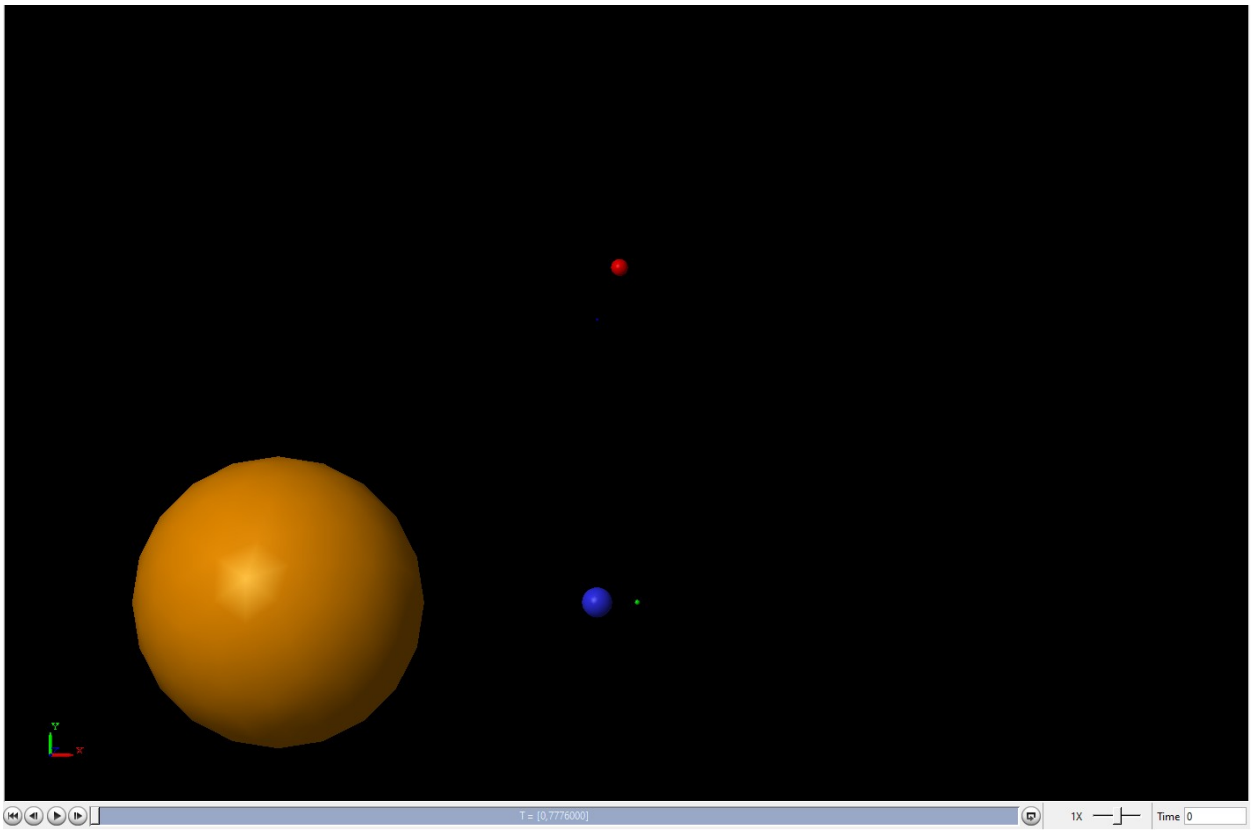

Figure 5.11: Top-view Screenshot of 3-D simulation at t = 0 secs

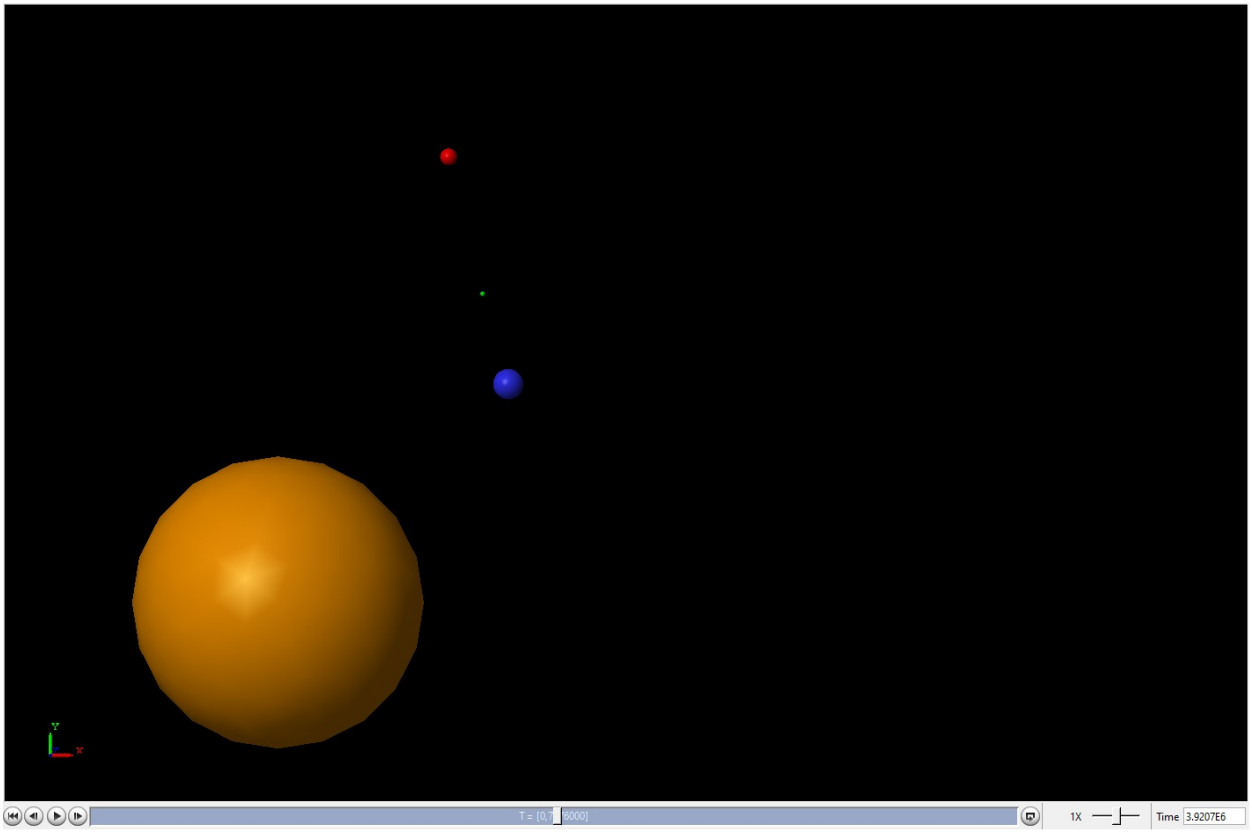

Figure 5.12: Top-view Screenshot of 3-D simulation at t = 3.9207E6 secs or ~ 45 days

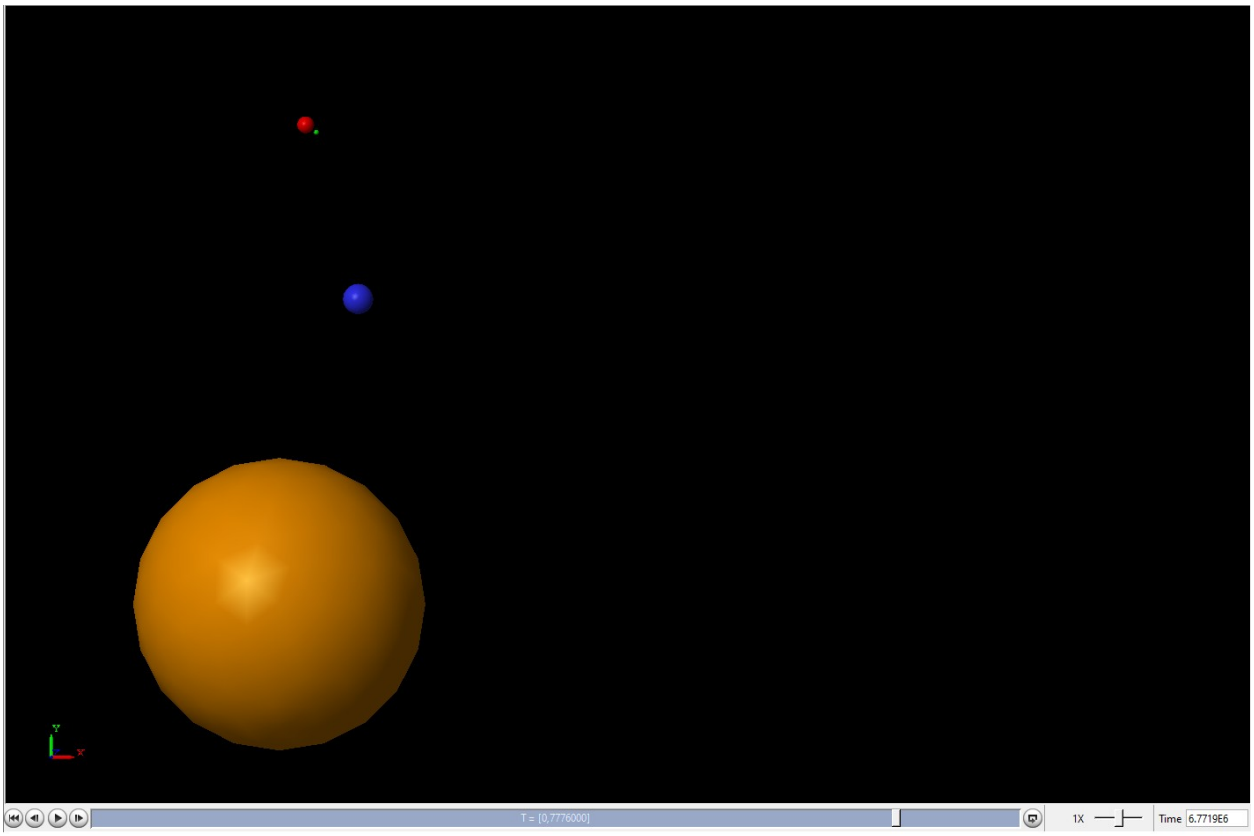

Figure 5.13: Top-view Screenshot of 3-D simulation at t = 6.7719E6 secs or ~ 78 days

The simulation for configuration III shows the spacecraft approaching Mars' orbit from the trailing end but that is due to the accelerated travel time and more parabolic orbit. This configuration appears to adhere more to a Mars flyby scenario or perhaps even gravity assist in course correction as the spacecraft can merely 'kiss' Mars. However, as stated in section 5.3, with a recalculated Mar's phase angle shift, orbit intersection may occur earlier, though once again not to a significant degree, and with a more desirable approach vector.

CHAPTER 6

CONCLUSION AND FUTURE WORK

The application of the VASIMR engine proves to be greatly effective in reducing the required travel time for missions to mars and with some research and development in nuclear electric power sources, could become a viable option for long distance space travel. However; it is evident that addition of multiple VASIMR engines undergoing continuous thrust simultaneously offers little increase in efficiency in reducing travel time; difference in configuration I and configuration III being only 12 days, only a 13% decrease. The next step would be to incorporate throttling by calculating multiple continuous burns of thrust at various stages to further accelerate the spacecraft. Under such a configuration it may perhaps be possible to travel to Mars in a matter of days or weeks rather than months [22].

Presently the VASIMR engine is still undergoing exhaustive testing to prove durability and long term reliability. In the next few months, testing will begin that consists of extensive burns of thrust in excess of 100 hours to demonstrate throttling capability and ensure that the engine itself can have a significant lifespan [22]. The next step will be planning and carrying out a technological mission to prove VASIMR's function in reality. Further astrodynamics analysis can be performed with extensive burn times and variable throttling to improve efficiency.

BIBLIOGRAPHY

[1] Longmier B.W., Squire J.P., Olsen C.S., Cassady L.D., Ballenger .G., Carter M.D., Ilin A.V., Glover T.W., McCaskill G.E., Chang Díaz F.R., Bering E.A. "Improved Efficiency and Throttling Range of the VX- 200 Magnetoplasma Thruster", *Journal of Propulsion and Power,* 30, No. 1, pp. 123-132, (2014).

[2] Jared P. Squire, Mark D. Carter, Franklin R. Chang Díaz, Matthew Giambusso, Andrew V. Ilin, Christopher S. Olsen, "Development toward a spaceflight capable VASIMR® engine and SEP applications", AIAA Space and Astronautics Forum and Exposition (SPACE 2014) AIAA 2014-4173 4 - 7 August 2014, San Diego, California (2014)

[3] Squire J.P., Carter M.D., Chang Díaz F.R., Giambusso M., Glover T.W., Ilin A.V., Oguilve Araya J., Olsen C.S., Bering E.A., Longmier B.W. "VASIMR® Spaceflight Engine System Mass Study and Scaling with Power", IEPC-2013-149, 33rd International Electric Propulsion Conference, The George Washington University, Washington, D.C., October 6-10, (2013).

[4] Castro Nieto J.A., Del Valle J., Martínez C., Rivera A., Oguilve J., Olsen C.S., Giambusso M., Carter M.D., Squire J.P., Chang Díaz F.R. "VASIMR® VX-CR Experiment: Status, Diagnostics and Plasma Plume Characterization", IEPC-2013-202, 33rd International Electric Propulsion Conference, The George Washington University, Washington, D.C., October 6-10, (2013).

[5] Chang Díaz F.R., Carter M.D., Glover T.W., Ilin A.V., Olsen C.S., Squire J.P., Litchford R.J., Harada N., Koontz S.L. "Fast and Robust Human Missions to Mars with Advanced Nuclear Electric Power and VASIMR Propulsion", Proceedings of Nuclear and Emerging Technologies for Space, Albuquerque, NM, February 25-28, (2013).

[6] Longmier B.W., Squire J.P., Cassady L. D., Ballenger M. G., Carter M. D., Olsen C. S., Ilin A. V., Glover T.W., McCaskill G. E.,Chang-Diaz F.R., Bering E. A., Del Valle J. "VASIMR® VX-200 Performance Measurements and Helicon Throttle Tables Using Argon and Krypton", IEPC-2011-156, Presented at the 32nd International Electric Propulsion Conference, Wiesbaden, Germany, September 11 – 15, 2011, (2011)

[7] Squire J.P., Olsen C. S., Chang-Diaz F.R., Cassady L. D., Longmier B.W., Ballenger M. G., Carter M. D., Glover T.W., McCaskill G. E., Bering E. A. "VASIMR® VX-200 Operation at 200 kW and Plume Measurements: Future Plans and an ISS EP Test Platform", IEPC-2011-156, Presented at the 32nd International Electric Propulsion Conference, Wiesbaden, Germany, September 11 – 15, (2011).

[8] Ilin, A.V., Cassady, L.D., Glover, T.W., Chang Díaz, F.R. "VASIMR® Human Mission to Mars", Space, Propulsion & Energy Science International Forum, March 15-17, University of Maryland, College Park, MD, (2011)

[9] Bering E.A., Longmier B.W., Glover T.W., Chang-Díaz F.R., Squire J.P., Carter M.D., Cassady L.D., Olsen C.S., McCaskill G.E., Chancery W.J. "VASIMR® VX-200: High power electric propulsion for space transportation beyond LEO", AIAA-2009-6481, AIAA Space 2009 Conference and Exposition, Pasadena, CA, September 14-17, (2009).

[10] Bering E., Longmier B., Glover T., Chang-Díaz F., Squire J., Brukardt M. "High power electric propulsion using VASIMRTM: Results from Flight Prototypes", AIAA-2009-245, 47th AIAA Aerospace Sciences Meeting, Orlando, FL, 5-8 January, (2009).

[11] E. Bering, B. Longmier, F. Chang Díaz, J. Squire, V. Jacobson, and M. Brukardt, "VASIMR VX-100 Engine: Next step to high power electric propulsion", in Proceedings of the 46th AIAA Aerospace Sciences Meeting and Exhibit, AIAA-2008-1087, Reno, NV, 7-10 January, (2008).
[12] Bering E. A., Glover T. W., Chang-Diaz F. R., Squire J. P., Cassady L. D., Brukardt M. S., Longmier B. "VASIMRTM: A Private Enterprise Solution to Space Transportation Beyond LEO", AIAA-2007-6134, Space 2007, Long Beach, CA, Sep 18-20, (2007).
[13] Glover T.W., Chang Diaz F. R., Ilin A. V., and Vondra R. "Projected Lunar Cargo Capabilities of HighPower VASIMRTM Propulsion", 30th International Electric Propulsion Conference, Florence, Italy, Sep 17-20, (2007).
[14] David Williams, MDCM MSc, Andre Kuipers, MD, Chiaki Mukai, MD PhD, and Robert Thirsk, MDCM SM, "Acclimation during space flight: effects on human physiology", CMAJ. 2009 Jun 23; 180(13): 1317–1323, (2009).
[15] Setlow B. Richard, "The hazards of space travel", EMBO Rep. 2003 Nov; 4(11): 1013–1016, (2003)
[16] Cucinotta FA, Kim M-HY, Chappell LJ, Huff JL, "How Safe Is Safe Enough? Radiation Risk for a Human Mission to Mars". PLOS ONE 8(10): e74988. October 16, (2013).
[17] Brown, Dwayne, Webster, Jay, "NASA Prepares for first interplanetary CubeSats", JPL, a division of the California Institute of Technology in Pasadena, June 12, (2015).
[18] Witze, Alexander, "NASA Suspends Next Mission to Mars", Nature Magazine, December 22, (2015).
[19] Curtis, Howard D., *Orbital Mechanics for Engineering Students* 3rd ed. Waltham, Massachusetts: Butterworht-Heinemann, 2013
[20] Sutton, George W., and Arthur Sherman. *Engineering Magnetohydrodynamics*. New York: McGraw-Hill, 1965. Print.
[21] Hunter, Jeanine. *Aerospace Engineering 242: Astrodynamics*. San Jose, 2016 Print.
[22] Squire, Jared. Phone Interview. January 11/2017
[23] Matlab and System Identification Toolbox Release 2015a, The Mathworks, Inc., Natick, Massachusetts, United States.